

# A 5D, polarised, Bethe-Heitler event generator for $\gamma \rightarrow \mu^+\mu^-$ conversion

D. Bernard,  
LLR, Ecole Polytechnique, CNRS/IN2P3, 91128 Palaiseau, France

October 29, 2019

## Abstract

I describe a five-dimensional, polarised, Bethe-Heitler event generator of  $\gamma$ -ray conversions to  $\mu^+\mu^-$ , based on a generator for conversion to  $e^+e^-$  developed in the past. Verifications are performed from close-to-threshold to high energies.

*keywords:*

gamma rays, pair conversion, muon pairs, gamma factory, event generator, Bethe-Heitler, Geant4

## 1 Introduction

In the past I wrote an event generator of  $\gamma$ -ray conversions to an  $e^+e^-$  pair [1] that we used for the simulation of the HARPO experiment [2, 3]. The generator samples the exact, that is, five-dimensional, Bethe-Heitler differential cross section. Later I developed a new version of that code, the fortran model [4] of an algorithm appropriate to event generation in Geant4. The Geant4 toolkit is used for the detailed simulation of scientific experiments that involve the interaction of “elementary” particles with matter, in particular with a detector [5–7]. The generator has been made available as the G4BetheHeitler5DModel physics model of Geant4 since release 10.5 [8, 9], see also SubSubSect. 6.5.4 of [10].

A Gamma Factory project is being proposed at CERN in the photon energy range  $1 < E < 400$  MeV [11], with photon intensities orders of magnitude above that presently available. Such a facility could be a powerful source of muons by gamma-ray conversions to  $\mu^+\mu^-$ , and therefore also a powerful source of neutrinos. A precise simulation of photon conversion to muons pairs was therefore intensely desirable [12].

The  $\gamma \rightarrow \mu^+\mu^-$  physics model presently available in Geant4, *G4GammaConversionToMuons* is based on the algorithm described in [13] and in Sect. 6.7 of [10] and in references therein. The calculation makes use of high-energy approximations and the model has been verified above incident photon energies of 10 GeV.

In this note I characterise a modified version of the fortran model of conversions to  $e^+e^-$  documented in [4] for conversions to  $\mu^+\mu^-$  and that is valid down to threshold, either for

- conversions
  - on a nucleus (nuclear conversion)  $\gamma Z \rightarrow \mu^+\mu^- Z$ ;
  - on an electron (triplet conversion)  $\gamma e^- \rightarrow \mu^+\mu^- e^-$ .
- on a target in an atom, or on an isolated target (“QED”)

- for linearly polarised or non-polarised incident photons.

The differential cross section for conversions of non-polarised photons was obtained by Bethe & Heitler [14], and that to linearly polarised photons by [15–17]<sup>1</sup>. The final state is five-dimensional, even when the recoiling target cannot be observed. It, the final state, can be defined by the polar angles  $\theta_+$  and  $\theta_-$ , and the azimuthal angles  $\phi_+$  and  $\phi_-$ , of the negative lepton ( $-$ ) and of the positive lepton ( $+$ ), respectively, and the fraction  $x_+$  of the energy of the incident photon carried away by the the positive lepton,  $x_+ \equiv E_+/E$  (Table 1 of [4]).  $q$  is the momentum “transferred” to the target. In case conversion takes place in the field of an isolated nucleus or electron, the Bethe-Heitler expression is used, while when the nucleus or the electron is part of an atom, the screening of the target field by the other electrons of the atom is described by a form factor, a function of  $q^2$  [18] (nuclear) or [19] (triplet).

Please note that in contrast with Bethe-Heitler [14], I do not assume that the energy carried away by the recoiling target be negligible (compare the differential element of eq. (20) of [14] to that of eqs. (1)-(3) of [4]).

The differential cross section diverges at small  $q$  and, for high-energy leptons, in the forward direction ( $\theta \approx 0$ ). The  $1/q^4$  divergence is a particularly daunting nuisance as the expression for  $q$  involves several of the variables that describe the final state. The inconvenience for event generation is overcome as is usual in particle physics, by performing each step of the conversion (gamma-target  $\rightarrow$  recoiling target-pair; pair  $\rightarrow$  two leptons) in its own centre-of-mass frame (Sect. 3 of [4] and references therein).

The problem is then reduced to using the Von Neumann acceptance-rejection method (Sect. 40.3 of [24]) from a mock-up probability density function (pdf) that is the simple product of five independent pdfs, of five judiciously chosen variables  $x_i, i = 1 \dots 5$ .

## 2 Bounds

The bounds of  $x_i, i = 2 \dots 5$  are pretty straightforward and do not depend on the mass of the leptons, see Table 3 of [4]. For  $x_1$ , though, the bounds must be provided and they depend on the energy of the incident photon, see Fig. 1 of [4] for conversions to  $e^+e^-$ . The  $x_1$  bounds for conversions to  $\mu^+\mu^-$  are similar and are shown in Fig. 1.

For better readability, energy-variation plots are presented as a function of the available energy

$$E' = E - E_{\text{threshold}}, \quad (1)$$

where the energy threshold is

$$E_{\text{threshold}} = 2(m_\mu^2/M + m_\mu), \quad (2)$$

where  $M$  is the target mass.

- For triplet conversion to  $\mu^+\mu^-$ ,  $E_{\text{threshold}}$  is close to 43.9 GeV.
- For nuclear conversion to  $\mu^+\mu^-$ ,  $E_{\text{threshold}}$  ranges from 223.2 MeV for hydrogen targets down to almost  $2m_\mu \approx 211.3$  MeV for heavy nuclei.

The  $x_1$  bounds are clearly not quite optimal for triplet conversion and might be tightened a bit further separately. The CPU gain for routine Geant4 use would be small though, due to the  $1/Z$  suppression of triplet with respect to nuclear and due to the much higher threshold energy.

---

<sup>1</sup>The polarised differential cross section first obtained by [15] was put in Bethe-Heitler form by [16], after which a misprint was corrected by [17].

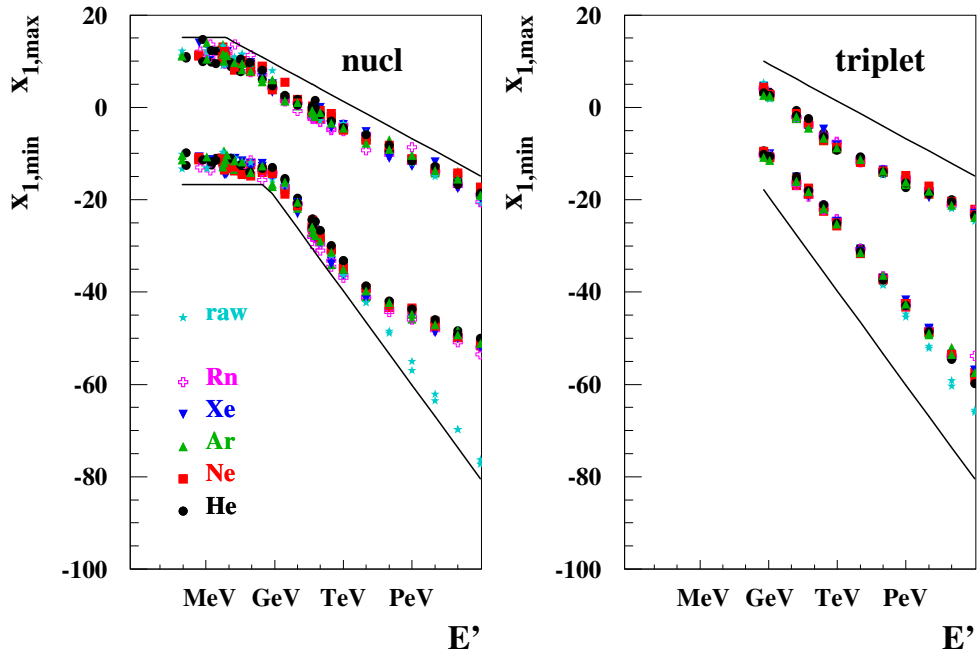


Figure 1: Variation with the available energy  $E'$  of the maximum and of the minimum values for variable  $x_1$ , for photon conversions to  $\mu^+\mu^-$ . Left: nuclear conversion; Right: triplet conversion. “raw” isolated charged target (star), and the following atoms: helium (bullet), neon (square), argon (upper triangle), xenon (down triangle) and radon (plusses). The lines denote the bounds that are used by the generator.  $P = 1$  and  $P = 0$  samples are plotted for each photon-energy value.

### 3 Maximum value of the differential cross section

The acceptance-rejection method needs the knowledge of the maximum value of the differential cross section, so as to determine a value of the constant  $C$  (see Sect. 5 of [4] or Sect. 40.3 of [24]). The variation of the maximum is shown in Fig. 2. As the maxima for all target masses were obtained from the same set of photon energies, and as the threshold varies with target mass for nuclear conversion, the available energy  $E'$  also varies with target mass. In the nuclear conversion plot, for example, for  $E = 217.40$  MeV photon conversion on helium,  $E_{\text{threshold}}$  is  $\approx 217.26$  MeV, that is,  $E' \approx 140$  keV. The parametrisation of the maximum is obtained with the same expression as for  $e^+e^-$  (eq. (9) of [4]) with a different set of parameters.

In practice, for safety,  $C$  is enlarged by a factor of 1.5 with respect to what can be seen on Fig. 2.

### 4 Distributions

Figs. 1 – 3 are based on samples of  $10^5$  simulated events, and Figs. 4 – 6 on samples of  $10^6$  simulated events. “Raw” nuclear samples, that is, simulations of conversions of an isolated target (“QED”) have been produced assuming an argon nucleus mass.

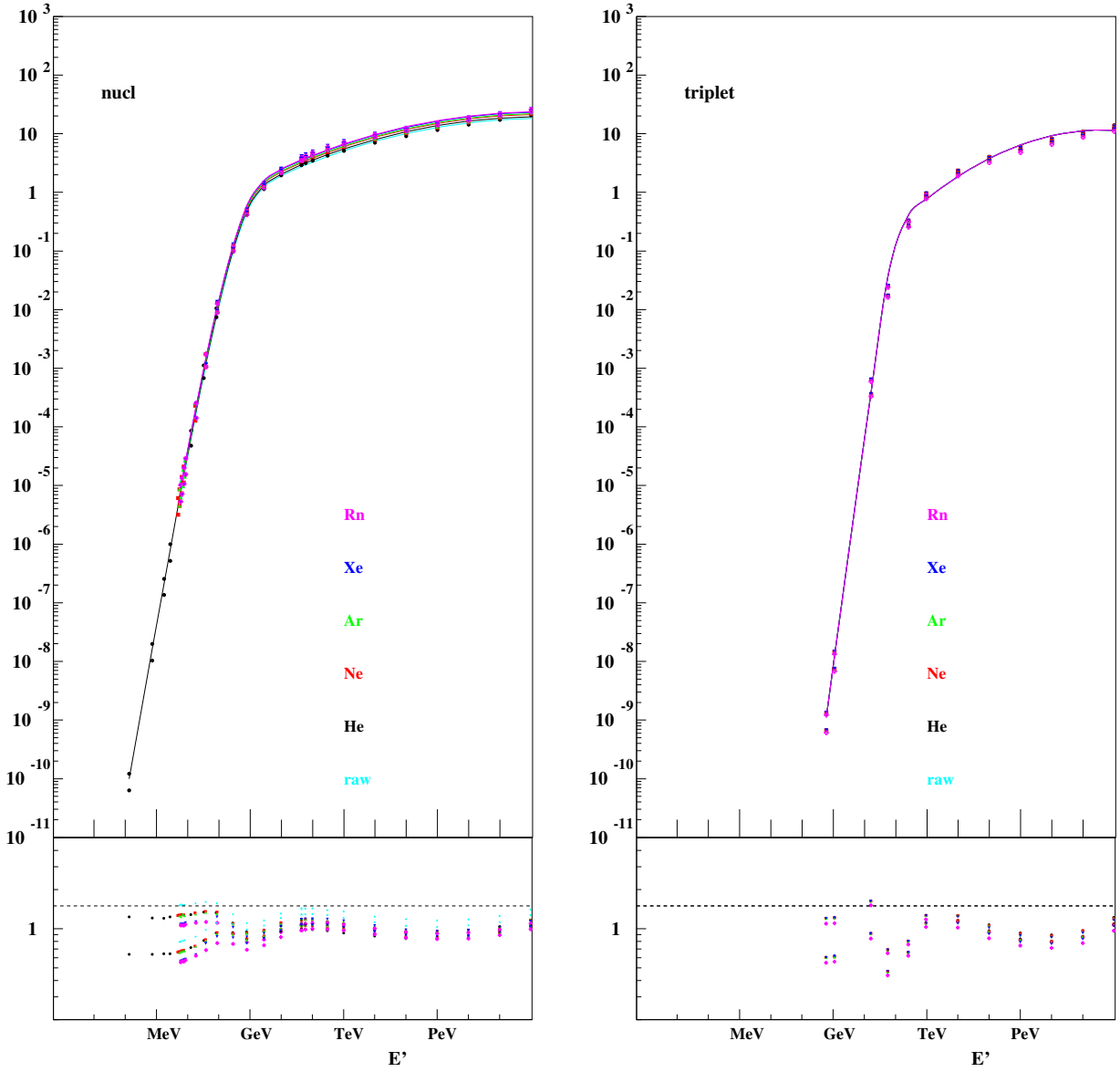


Figure 2: Top: Variation of the maximum value of the pdf (arbitrary units) with the available energy  $E'$ . Left: nuclear conversion; Right: triplet conversion. “raw” isolated charged target (star), and the following atoms: helium (bullet), neon (square), argon (upper triangle), xenon (down triangle) and radon (plusses). The curves denote the fit to the present data of the expression of eq. (9) of [4]. Bottom: residues of the fit, with the 1.5 safety factor marked with a dashed line.  $P = 1$  and  $P = 0$  samples are plotted for each photon-energy value.

#### 4.1 Polarisation asymmetry

The measurement of the polarisation angle  $\varphi_0$  and of the linear polarisation fraction  $P$  of a gamma-ray beam can be performed by the analysis of the distribution of the event azimuthal angle  $\varphi$

$$\frac{dN}{d\varphi} \propto (1 + AP \cos[2(\varphi - \varphi_0)]), \quad (3)$$

Figure 3 shows the polarisation asymmetry,  $A$ , obtained from the ( $P = 1$ ) samples, defining the event azimuthal angle as the bisector of the electron and of the positron azimuthal angles,  $\varphi \equiv (\phi_+ + \phi_-)/2$  [21], and using the moments' method [1, 20, 21].

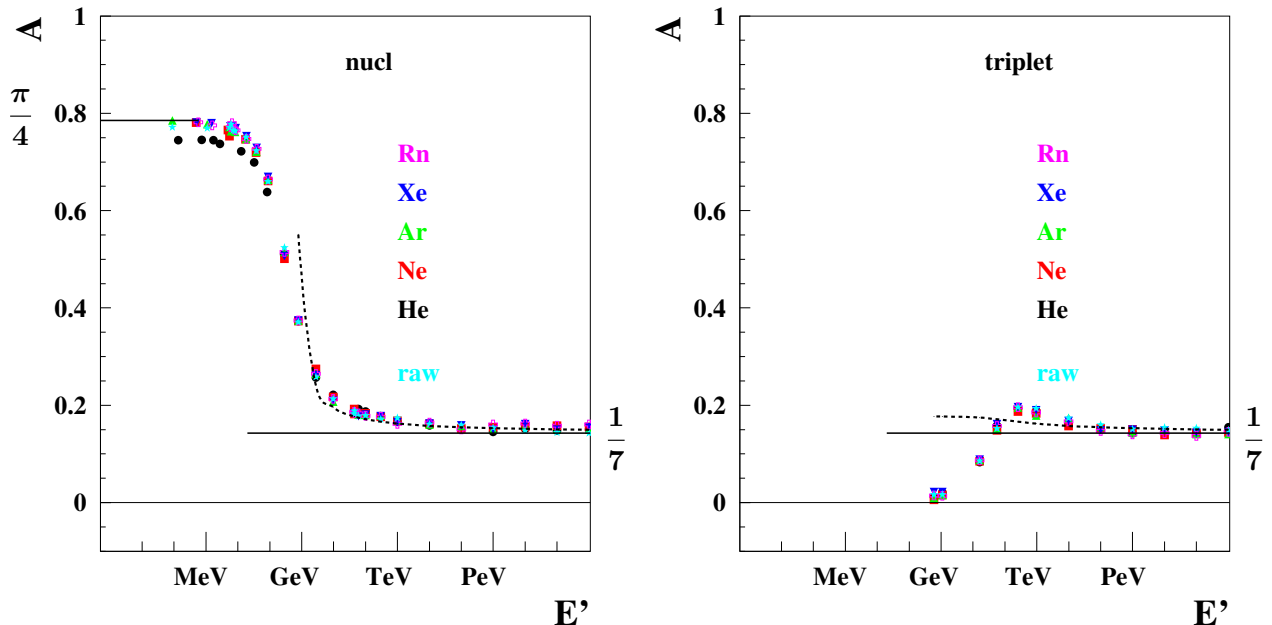


Figure 3: Polarisation asymmetry calculated on simulated event samples as a function of  $E'$ . Left: nuclear conversion. Right: triplet conversion. “raw” isolated charged target (star), and the following atoms: helium (bullet), neon (square), argon (upper triangle), xenon (down triangle) and radon (plusses). The horizontal lines denote the low- and high-energy approximations of  $\pi/4$  and  $1/7$ , respectively. The dashed curves denote the Boldyshev-Peresunko high-energy approximation [22] and shown here in eq. (4).

Results agree nicely with the Boldyshev-Peresunko asymptotic expression [22] at high energy:

$$A \approx \frac{\left(\frac{4}{9}\right) \log\left(\frac{2E}{m_\mu c^2}\right) - \left(\frac{20}{28}\right)}{\left(\frac{28}{9}\right) \log\left(\frac{2E}{m_\mu c^2}\right) - \left(\frac{218}{27}\right)}. \quad (4)$$

At low energy the obtained values agree with the asymptotic value of  $\pi/4$  obtained in [21] for nuclear conversion and for nuclei that are much heavier than a muon, mildly for helium, but tends to zero for triplet conversion.

## 4.2 Energy share

The distributions of the fraction  $x_+ \equiv E_+/E$  of the energy of the incident photon that is taken away by the positive lepton is shown in Fig. 4. They compare nicely with the published representations of the singly-differential cross section obtained by integration on all other variables (Fig. 5 of [14]).

## 4.3 Recoil momentum

The distribution of the ( $\log_{10}$  of the) recoil momentum is shown in Fig. 5.

## 4.4 Opening angle

Figure 6 shows the distributions of the pair opening angle,  $\theta_{+-}$ , normalised to  $1/E$  for conversions on argon. At high energies, they peak at the most probable value,  $\hat{\theta}_{+-}$ , computed by Olsen in the

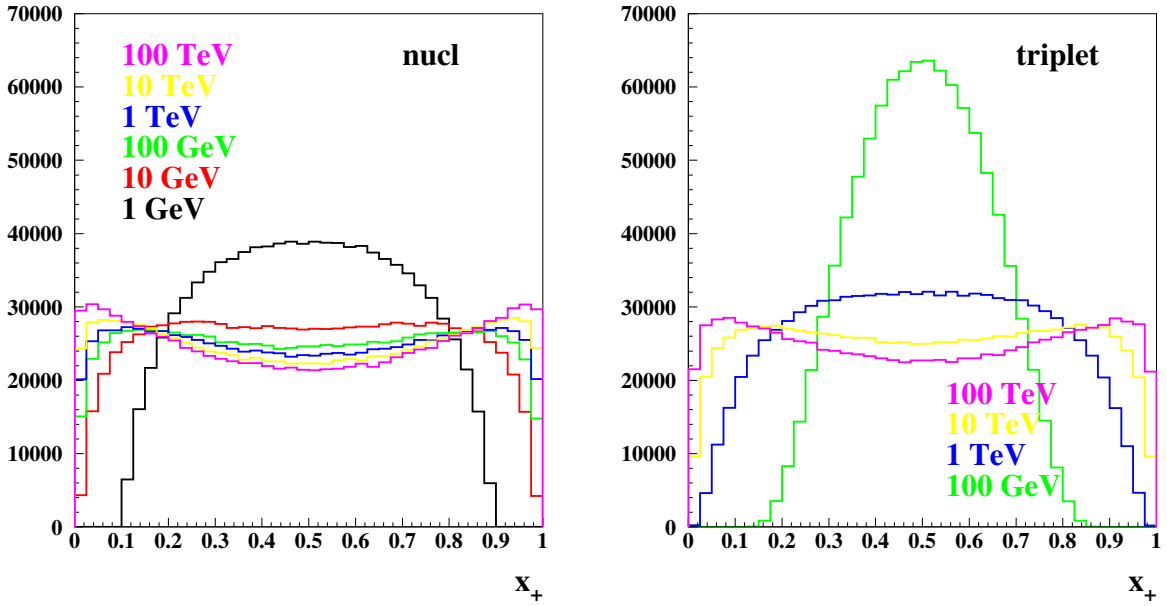


Figure 4: Distributions of the fraction of the energy of the incident photon that is taken away by the positive lepton,  $x_+ \equiv E_+/E$ , for various values of  $E$  (conversions on argon).

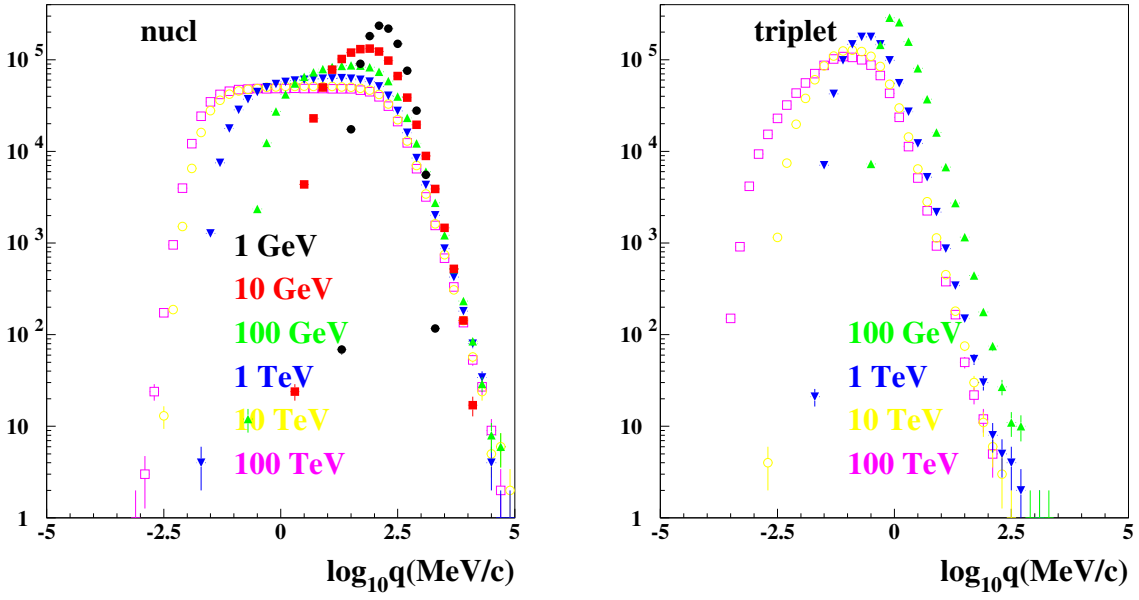


Figure 5: ( $\log_{10}$  of the) recoil momentum spectra for gamma conversions on argon atoms.

high-energy approximation [23], that is indicated by a vertical line:

$$\hat{\theta}_{+-} = \frac{3.2 mc^2}{E}, \quad (5)$$

where  $m$  is the mass of the pair lepton. Here  $m = m_\mu$  and

$$\hat{\theta}_{+-} \approx \frac{338.1 \text{ MeV}}{E}. \quad (6)$$

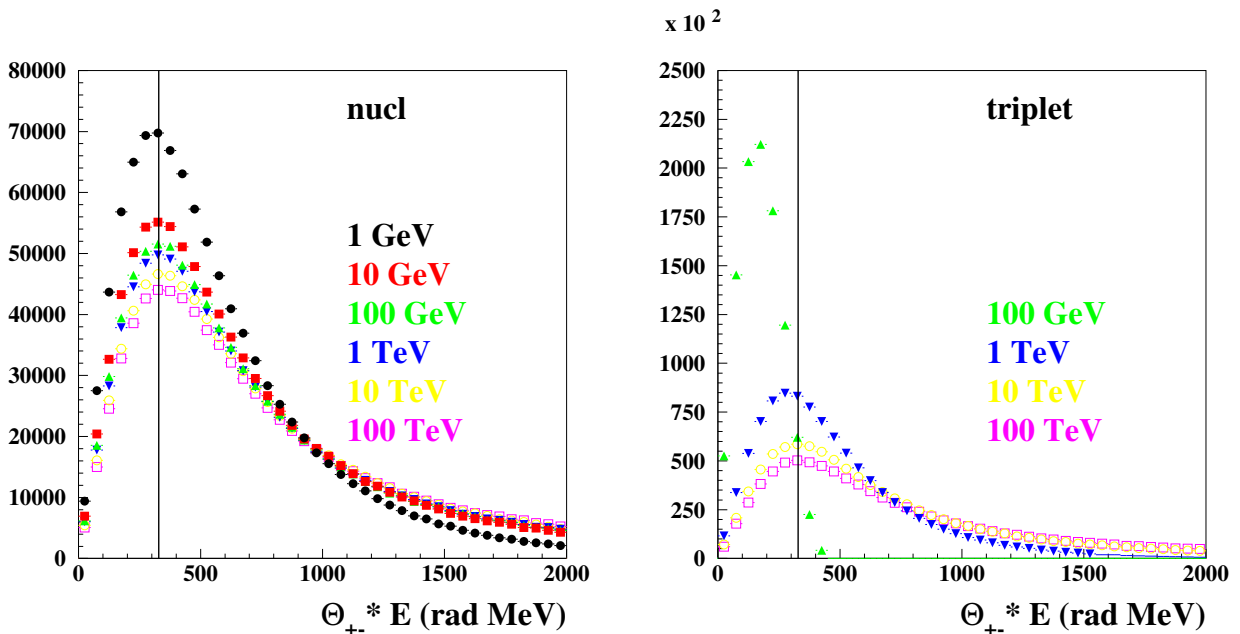


Figure 6: Distributions of the product of the pair opening angle and of the photon energy,  $\theta_{+-} \times E$ , for nuclear conversions on argon for 1 GeV (bullet), 10 GeV (full square), 100 GeV (upper triangle), 1 TeV (down triangle), 10 TeV (circles) and 100 TeV (empty squares). The vertical value shows the most probable value of  $\approx 338$ . rad  $\cdot$  MeV computed by Olsen in the high-energy approximation [23] (see also eqs. (5)-(6)).

## 5 Conclusion

I have adapted the sampler of the Bethe-Heitler differential cross section that I had written for gamma conversions to  $e^+e^-$  pairs [4] to the generation of gamma conversions to  $\mu^+\mu^-$ , by simply tuning the parametrisations of the bounds for variable  $x_1$  (Sect. 2) and of the maximum differential cross section (Sect. 3). Verifications of various distributions obtained by the algorithm have been performed successfully from threshold to PeV energies (Sect. 4).

The Geant4 physics model corresponding to the present algorithm is about to be made available to users in release 10.6 [25].

## 6 Acknowledgments

I'd like to express my gratitude to Vladimir Ivantchenko who brought the need for a correct low-energy  $\gamma \rightarrow \mu^+\mu^-$  event generator to my attention and to Igor Semeniouk and Mihaly Novak for stimulating discussions.

## References

- [1] D. Bernard, "Polarimetry of cosmic gamma-ray sources above  $e^+e^-$  pair creation threshold," Nucl. Instrum. Meth. A **729** (2013) 765.
- [2] P. Gros *et al.*, "Performance measurement of HARPO: A time projection chamber as a gamma-ray telescope and polarimeter," Astropart. Phys. **97** (2018) 10.

- [3] D. Bernard [HARPO Collaboration], “HARPO, a gas TPC active target for high-performance  $\gamma$ -ray astronomy; demonstration of the polarimetry of MeV  $\gamma$ -rays converting to  $e^+e^-$  pair,” Nucl. Instrum. Meth. A **936** (2019) 405.
- [4] D. Bernard, “A 5D, polarised, Bethe-Heitler event generator for  $\gamma \rightarrow e^+e^-$  conversion,” Nucl. Instrum. Meth. A **899** (2018) 85.
- [5] S. Agostinelli *et al.* [GEANT4 Collaboration], “GEANT4: A Simulation toolkit,” Nucl. Instrum. Meth. A **506** (2003) 250.
- [6] J. Allison *et al.*, “Recent Developments in Geant4,” Nucl. Instrum. Meth. A **835** (2016) 186.
- [7] J. Apostolakis *et al.*, “Progress in Geant4 Electromagnetic Physics Modelling and Validation,” J. Phys. Conf. Ser. **664** (2015) 072021.
- [8] I. Semeniouk and D. Bernard, “C++ implementation of Bethe-Heitler, 5D, polarized,  $\gamma \rightarrow e^+e^-$  pair conversion event generator,” Nucl. Instrum. Meth. A **936** (2019) 290.
- [9] V. Ivanchenko *et al.*, “Progress of Geant4 electromagnetic physics developments and applications”, EPJ Web of Conferences **214**, 02046 (2019).
- [10] Geant4 Physics Reference Manual, Release 10.5, March 5 2019 (Geant4 User Documentation).
- [11] M. Krasny *et al.*, “The CERN Gamma Factory Initiative: An Ultra-High Intensity Gamma Source,” 9th International Particle Accelerator Conference, Vancouver, Canada, 29 Apr - 4 May 2018, doi:10.18429/JACoW-IPAC2018-WEYGBD3.
- [12] V. Ivantchenko, “Muon pair production Monte Carlo”, Gamma Factory meeting, CERN, 25-28 March 2019 (indico).
- [13] H. Burkhardt, S. R. Kelner and R. P. Kokoulin, “Monte Carlo generator for muon pair production,” CERN-SL-2002-016-AP, CLIC-NOTE-511.
- [14] H. Bethe and W. Heitler, “On the Stopping of Fast Particles and on the Creation of Positive Electrons”, Proceedings of the Royal Society of London A, **146** (1934) 83.
- [15] T. H. Berlin and L. Madansky, “On the Detection of gamma-Ray Polarization by Pair Production”, Phys. Rev. **78** (1950) 623.
- [16] M. M. May, “On the Polarization of High Energy Bremsstrahlung and of High Energy Pairs”, Phys. Rev. **84** (1951) 265.
- [17] Jauch and Rohrlich, *The theory of photons and electrons*, (Springer Verlag, 1976).
- [18] N.F. Mott, H.S.W. Massey, “The Theory of Atomic Collisions”, University Press, Oxford, 1934.
- [19] J.A. Wheeler and W.E. Lamb, “Influence of atomic electrons on radiation and pair production”, Phys. Rev. **55** (1939) 858 (errata in **101** (1956) 1836).
- [20] P. Gros *et al.* [HARPO Collaboration], “ $\gamma$ -ray telescopes using conversions to  $e^+e^-$  pairs: event generators, angular resolution and polarimetry,” Astropart. Phys. **88** (2017) 60.
- [21] P. Gros *et al.* [HARPO Collaboration], “ $\gamma$ -ray polarimetry with conversions to  $e^+e^-$  pairs: polarization asymmetry and the way to measure it,” Astropart. Phys. **88** (2017) 30.
- [22] V. F. Boldyshev and Y. P. Peresunko, “Electron-positron pair photoproduction on electrons and analysis of photon beam polarization,” Yad. Fiz. **14** (1971) 1027.
- [23] H. Olsen, “Opening Angles of Electron-Positron Pairs,” Phys. Rev. **131** (1963) 406.
- [24] M. Tanabashi *et al.* [Particle Data Group], “Review of Particle Physics,” Phys. Rev. D **98** (2018) 030001, on pdglive.
- [25] I. Hřivnácová for the Geant4 EM working group, “Geant4 electromagnetic physics progress”, the 24th International Conference on Computing in High-Energy and Nuclear Physics (CHEP 2019), 4 - 8 Nov. 2019, Adelaide, Australia.